




Increasing Power Output of Quantum Cascade Lasers (QCLs) Added with AlAs/InAs Layers Through Bandgap Engineering

Shigeyuki Takagi¹^a, Hiroataka Tanimura¹^b, Tsutomu Kakuno², Rei Hashimoto², Kei Kaneko² and Shinji Saito²^c

¹*Department of Electrical and Electronics Engineering, School of Engineering, Tokyo University of Technology, 1404-1 Katakura, Hachioji, Tokyo, Japan*

²*Corporate Manufacturing Engineering Center, Toshiba Corporation, 33 Shinisogo, Isogo, Yokohama, Kanagawa, Japan*

Keywords: Quantum Cascade Lasers, QCLs, Active Region, Injection Region, Bandgap Engineering, Nonequilibrium Green's Function, Gain, Wavelength, Simulation, Quantum Well.


Abstract: We applied bandgap engineering to n-type semiconductor quantum cascade lasers (QCLs) and investigated the effects the following methods to increase the power output of structures reported in the literature. Three types of structure were investigated: (1) the AlAs/InAs structure that promotes the formation of population inversion by promoting electron transport leakage, (2) the structure with a thin barrier layer that enhances electron transport, and (3) the structure with an active region with reduced Al composition that assists in the formation of population inversion. The gains and wavelengths of these structures were calculated using a simulator that uses a nonequilibrium Green's function. The results showed that the AlAs/InAs structure had the highest gain. On the basis of the simulation results, two types of QCL, the reference structure and the AlAs/InAs, structure were fabricated. The peak output of the laser in the AlAs/InAs structure increased 1.73 times, compared with that in the reference structure. The validities of investigating the increase in power output by bandgap engineering and simulating QCL characteristics were demonstrated.


1 INTRODUCTION


Quantum cascade lasers (QCLs) are n-type semiconductor lasers in which two types of semiconductor film are alternately stacked, and the laser light in the infrared region can be obtained (Faist et al., 1994). Since the wavelength of QCLs is in the infrared region, QCLs are expected to be applied to trace gas analysis and remote gas detection (Faist et al., 2016). With such trace substance detection and gas detection at a distance, higher sensitivity is expected by increasing the output. Since the amount of a laser absorption is measured in the detection of trace substances, it is necessary to propagate a long optical path. To increase the output of lasers, it is effective to utilize simulation and bandgap engineering. High-precision simulation is required to evaluate the effect of the band structure considered with bandgap engineering.

As shown in Fig.1, a QCL consists of injection regions that transport electrons and active regions that have several pairs of barrier and well layers. Laser light is emitted when electrons transition from the upper level to the lower level in the quantum well formed in an active region. In the current simulators, the Schrödinger equation is solved to calculate the wave function, and the rate equation method is applied to the two energy levels at which the laser is emitted.

In the simulators, the amount of light emitted is calculated semiclassically from the lifetimes of the upper and lower levels and the transition probability between the upper and lower levels (Lu et al., 2006). In contrast, calculations using nonequilibrium Green's functions allow the distribution of electron density and the transition of electrons from the upper to lower levels to be calculated quantumly (Grange, 2015). Using this method, we have obtained an active

^a <https://orcid.org/0009-0009-6444-8748>

^b <https://orcid.org/0000-0002-7653-4602>

^c <https://orcid.org/0000-0002-1829-6482>

layer structure that enhances the light emission intensity (Tanimura et al., 2022).

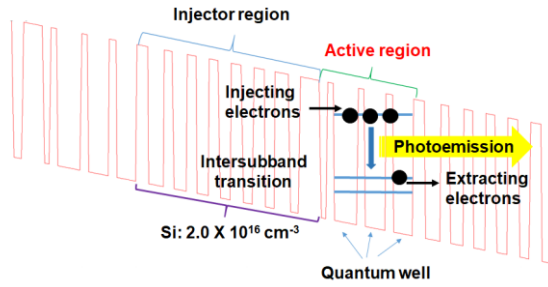


Figure 1: Band structure of typical QCL (Tanimura 2022).

In this study, a simulator of nonequilibrium Green's functions was used to verify bandgap engineering. Bandgap engineering is a technique for improving the performance of semiconductor properties manipulating band structures. We attempted to increase the output power of QCLs reported in the reference through bandgap engineering (Capasso, 1987), (Chaves et al., 2020). To increase the output power, we considered three types of structure: (1) the AlAs/InAs structure that promotes the formation of a population inversion by promoting electron transport leakage, (2) the structure with a thin barrier layer that enhances electron transport, and (3) structure with an active region with reduced Al composition that assists in the formation of population inversion.

Gains and wavelengths were calculated using a simulator with nonequilibrium Green's functions, and it was shown that the AlAs/InAs structure had the highest gain. On the basis of the simulation results, two types of QCL, a reference structure (baseline structure) and an AlAs/InAs structure, were fabricated. We report that the peak output of the laser in the AlAs/InAs structure increased 1.73 times compared with that in the reference structure.

2 QCL SIMULATION

2.1 QCL Simulator Incorporating Nonequilibrium Green's Functions

The simulator used in this study was nextnano.QCL (nextnano, Inc.) (Grange, 2015). The calculation flow in the simulator is shown in Fig. 2. In the Schrödinger equation, assuming that the unperturbed Hamiltonian is H_0 and the electron scattering is the perturbation term Hamiltonian H_{scatt} , the Hamiltonian H of the system is given by equation (1).

$$H = H_0 + H_{SCATT} \quad (1)$$

Using this Hamiltonian, the Schrödinger equation is solved to calculate the electron trajectory.

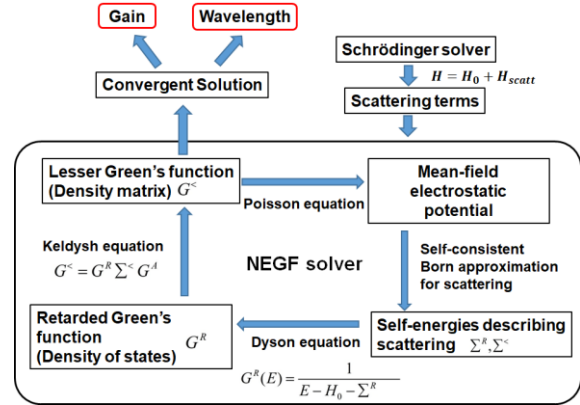


Figure 2: QCL simulator incorporating nonequilibrium Green's function (Tanimura, 2022).

The Poisson equation is then solved to obtain the mean-field electrostatic potential, and the retardation self-energy Σ^R and Lesser self-energy $\Sigma^<$ that describe the electron scattering are calculated. The density of states (DOS) is calculated from the retardation Green's function G^R using the Dyson equation, equation (2).

$$G^R = \frac{1}{E - H_0 - \Sigma^R} \quad (2)$$

The electron density matrix is calculated from the Lesser Green's function $G^<$ using the Keldysh equation shown in equation (3).

$$G^< = G^R \Sigma^< G^A \quad (3)$$

Here, G^A stands for the advanced Green's function. From the obtained electron density matrix, the current and gain are obtained.

From a series of calculations, we calculate the relationship between the emitted energy (wavelength) and the gain. We estimated that the wavelength at which the gain is maximum is the laser oscillation wavelength. By using the nonequilibrium Green's function, it is possible to add the effects of the crystal lattice and electron scattering. This makes it possible to perform calculations that take into account the scattering of electrons, and crystal lattice, factors such as corresponding to the operating temperature and film stress depending on the film composition in QCLs.

2.2 Verification of Simulation Accuracy

To estimate the validity of this simulator, the QCL film structure reported by Evans et al. was input into the simulator (Evans et al., 2007). The film structure was modelled with two pairs of injector and active regions, and the film composition and thickness were the values given in the paper. The maximum gain intensity obtained in the simulation, which was assumed to be the laser oscillation wavelength, and was compared with the oscillation wavelength reported in the paper. In the calculation, the voltage V_{ap} applied to one pair of injector and active regions was set to 400 mV.

Figure 3 shows the calculation results. Figure 3 (a) is the gain intensity, and Fig. 3(b) shows DOS distribution. The horizontal axes in Figs. 3(a) and (b) indicate the position of the QCL film. In Fig. 3(a), a high gain is observed at the position corresponding to the active region. The photon energy of this gain is 260 meV, which corresponds to an optical wavelength of 4.77 μm . The oscillation wavelength in the experiment of Evans et al. was 4.71 μm , which is in good agreement with the calculation results using nextnano.QCL.

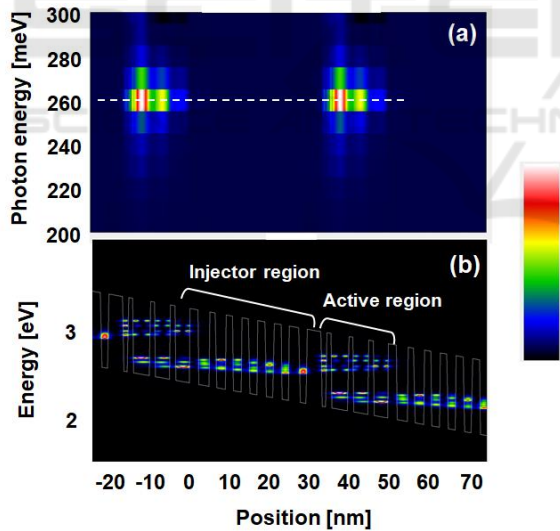


Figure 3: Simulation results. (a) gain and (b) DOS distributions (Tanimura, 2022).

In Fig. 3(b), there are two stages of electron distribution in the active region, and the upper and lower electron distribution regions correspond to the upper and lower levels of laser oscillation. In addition, electrons with almost the same energy level are distributed in the injector region, which indicates that electrons propagate through the injector region.

It was shown that nextnano.QCL can accurately model the electron propagation and the emission of laser light, and can obtain the same oscillation wavelength as the experimental results.

3 INCREASING POWER OUTPUT WITH BANDGAP ENGINEERING

3.1 Bandgap Engineering for QCLs

Figure 4 shows the evaluated band structures. Figure 4(A) is the band structure reported in the paper (Evans et al., 2007). In the reference, all layers in the injection region were doped with Si at a concentration of $1 \times 10^{16} \text{ cm}^{-3}$. In contrast, in Fig. 4(A), only the four layers in the injection region were doped with Si at a concentration of $1 \times 10^{17} \text{ cm}^{-3}$, as shown in the figure. The QCL is formed by alternately stacking two types of film, $\text{In}_{0.52}\text{Al}_{0.48}\text{As}$ (InAlAs) and $\text{In}_{0.53}\text{Ga}_{0.47}\text{As}$ (InGaAs).

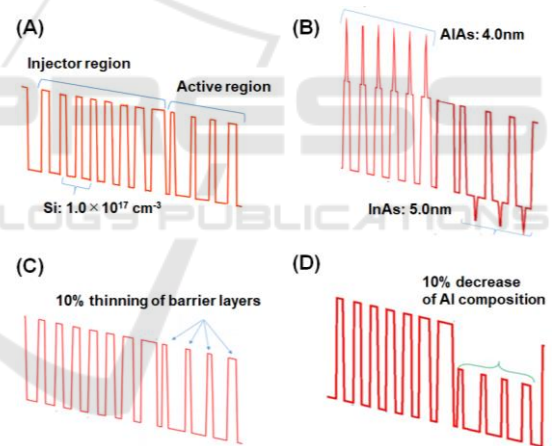


Figure 4: Bandgap engineering. (A) baseline structure, (B) AlAs/InAs structure, (C) structure with thin barrier layer, and (D) structure with active region with reduced Al composition.

In addition, by applying a negative voltage to the injection region side, the band of the QCL is tilted so that the left side of Fig. 4(A) is higher. We call the three quantum wells in the active region the first quantum well, the second quantum well, and the third quantum well from the left in Fig. 4(A). In the field of semiconductors, bandgap engineering is performed to improve the performance of semiconductors based on band structures (Capasso, 1987), (Chaves et al., 2020). We applied bandgap engineering to this

structure and considered the following three types of band structures.

Structure (B) in Fig. 4 is a band structure to increase the electron transport in the injection region and the population inversion in the active region. Electrons pass through the injection region by the tunnel effect. The energy difference between the InAlAs layer and the InGaAs layer is 0.52 eV (Hybertsen, 1991), and electrons pass through near the middle of this energy difference. On the other hand, at a room temperature of 27°C, the thermal energy is 0.026 eV, and electrons with large thermal fluctuations jump out of the upper level. To suppress this phenomena, AlAs layers are added to the center of InAlAs layers. The upper levels of AlAs layers were higher than those of InAlAs layers, and protruding levels above the band are formed, as shown in Fig.4(B). The higher upper level reduces electron leakage during transport.

Furthermore, in the active layer, a 5.0nm-thick InAs layer was added to the lower level InGaAs layer. This generates a protruding lower level. In the active layer, the laser is excited by the transition of electrons from the upper level to the lower level in the quantum well. The addition of a protruding level to the lower energy level widens the bottom of the lower level, increasing the probability of transition from the upper level to the lower level.

(C) and (D) in Fig.4 are band structures that improve the electron transport in the active region. In the band diagram of (A), three consecutive quantum wells are formed, and in the simulation results in Fig. 3(b), a population inversion is seen in the first to third quantum wells. If electrons from the injection region are efficiently transported, the upper level electron density can be increased in the three quantum wells. In (C), the film of the barrier layer in the active region is made 10% thinner to improve the electron transport efficiency. In the band structure of (D), we expect the InAlAs layers in the active region to have low energy levels, and for electrons leaking out of the barrier layers to contribute to population inversion in the adjacent quantum wells. The energy level of the InAlAs film is lowered by reducing the Al concentration (Hybertsen, 1991). In (D), the Al composition was reduced by 10%. In this study, we call (A) the baseline structure (A) and (B)–(D) the improved structures.

3.2 Simulation Results

Figure 5(b) shows the calculation results of the electron density for the band structure (B) in Fig. 4. The V_{ap} applied to one pair of injection region and

active regions was set to 400 mV. For reference, Fig. 5(a) shows the electron density distribution for the baseline structure (A) calculated under the same conditions. The electron density of the upper and lower levels in the quantum wells of structure (B) is higher than that of structure (A). In particular, from the high electron density in the upper level in the third quantum well, it is expected that many electrons will be transported from the first quantum well to the third quantum well, exciting the laser light.

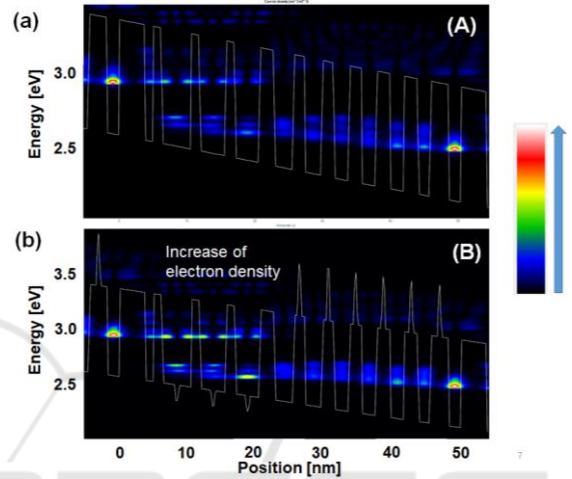


Figure 5: Electron distributions in simulation results. (A) baseline structure and (B) AlAs/InAs structure.

Next, the gains and wavelengths were calculated for baseline structure (A) and improved structure (B) by changing V_{ap} from 350 to 550 mV. The calculation results are shown in Fig. 6. Improved structure (B) has a higher gain at all V_{ap} values. In addition, the gains in the structure (A) and structure (B) at $V_{ap} = 400$ mV were 42.4 cm^{-1} and 63.6 cm^{-1} , respectively. Improved structure (B) achieved a gain 1.5 times greater than that of the standard structure (A). Figure 5(b) shows the calculation results for the wavelengths of the baseline structure (A) and improved structure (B).

In the V_{ap} range of 400 to 500 mV, the wavelength of baseline structure (A) was $4.96 \mu\text{m}$ and that of the improved structure (B) was $4.77 \mu\text{m}$. It is estimated that the improved structure increased the energy difference between the upper and lower levels, resulting in a shorter wavelength. As mentioned in Section 3.1, In Evans's reference (Evans, 2007), all layers in the injection region were doped with Si at a concentration of $1 \times 10^{16} \text{ cm}^{-3}$. In contrast, in Fig. 4(A), only the four layers in the injection region were doped with Si at a concentration of $1 \times 10^{17} \text{ cm}^{-3}$. We estimated that this difference in the structure of QCLs causes the difference between the oscillation

wavelength calculated in Section 2.2 (4.77 μm) and that calculated in this section (4.97 μm).

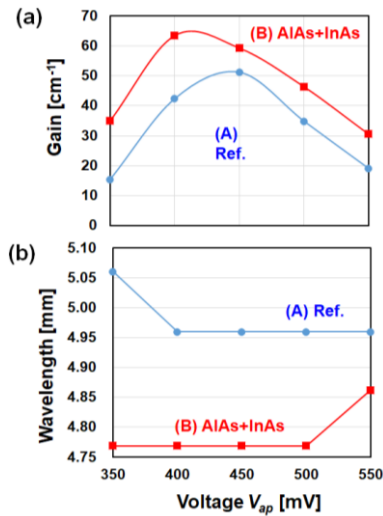


Figure 6: Simulation results. (a) gain and (b) wavelength.

The gains and wavelengths were calculated by changing V_{ap} from 350 to 550 mV. At $V_{ap} = 400$ mV, the gain of baseline structure (A) was set as 100%, and the gains of improved structures (C) and (D) relative to that of structure (A) were calculated. The calculation results are shown in Fig. 7. The gain of improved structure (C) was 117%, and that of the improved structure (D) was 126% compared with that of structure (A). Among structures (A) to (D), improved structure (B) had the highest gain of 150%. On the basis of these results, we decided to fabricate prototype QCLs with structure (A) and improved structure (B) and compared the laser outputs and wavelengths of the two QCLs.

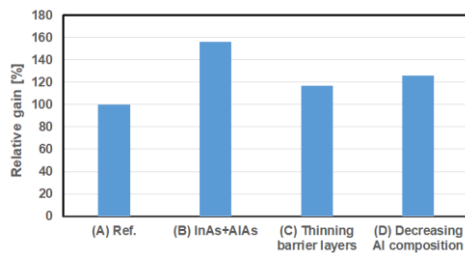


Figure 7: Gains of four types of band structure.

4 PROTOTYPE AND EVALUATION OF QCLs

The left part of Fig. 8 shows a photograph of the prototype QCLs, and the middle and right parts of the

figure shows the tip length, ridge width, and band structure of the QCLs. The band structures of baseline structure (A) and improved structure (B) were the same as those in Chapter 3. The ridge, which limits the width through which current flows and increases the current density, was determined to be 12 μm for the standard structure (A) and 15 μm for improved structure (B), owing to differences in prototype lots. Since the difference in ridge width results in a difference in current density, the current of improved structure (B) with a wider ridge was estimated to be higher than that of baseline structure (A). The prototype QCL chip was mounted on a C-mount, as shown in the left part of Fig. 8.

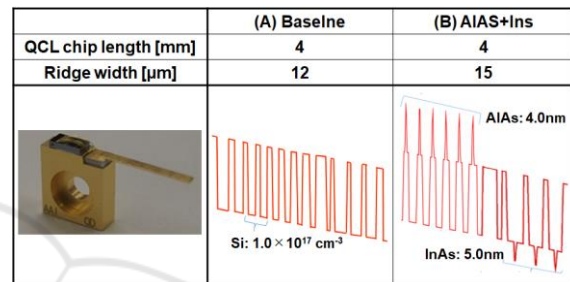


Figure 8: Photograph, tip length, ridge width, and band structure for the prototyped QCLs.

The QCL device was cooled to 77 K by liquid nitrogen and operated with a pulse width of 300 ns and a repetition rate of 100 kHz. Figure 9(a) shows the relationship between the current density and the peak applied voltage, and Fig. 9(b) shows the relationship between the current density and the laser output. In the case of Fig 9(a), the current begins to flow when the voltage applied to the device exceeds 10 V for both baseline structure (A) and improved structure (B). The applied voltage to obtain the same current density is higher for improved structure (B). The applied voltages of baseline structure (A) and improved structure (B) at a current density of 2 kA/cm^2 were 14.1 V and 17.0 V, respectively. This means that the voltage for the improved structure (B) is 1.2 times higher than that of the reference structure (A). This corresponds to the ridge width of the improved structure (B) being 1.25 times that of the baseline structure (A).

In Fig. 9(b), the laser outputs of baseline structure (A) and improved structure (B) increase with current density. The laser output of baseline structure (A) saturated at 3.22 kA/cm^2 , and a maximum output of 203.7 mW was obtained. On the other hand, improved structure (B) obtained a maximum output of 352.3 mW at a current density of 2 kA/cm^2 . The maximum output of improved structure (B) was 1.73 times that

of baseline structure (A). The laser output of improved structure (B) did not show any tendency to saturate with increasing current density, and it was suggested that a higher laser output could be obtained by increasing the current density.

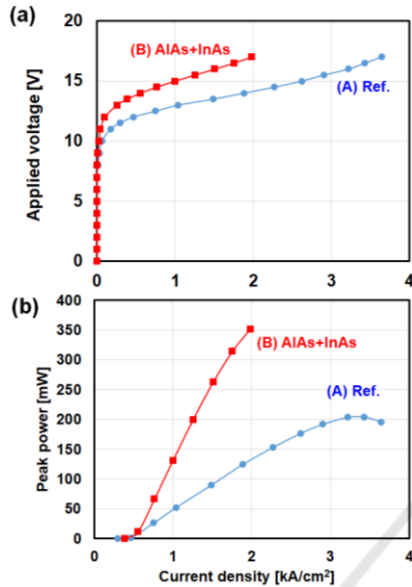


Figure 9: Measurement results of QCL characteristics. (a) I-V curve and (b) laser output peak power.

Figure 10 shows the measurement results of the lasing wavelengths of baseline structure (A) and improved structure (B).

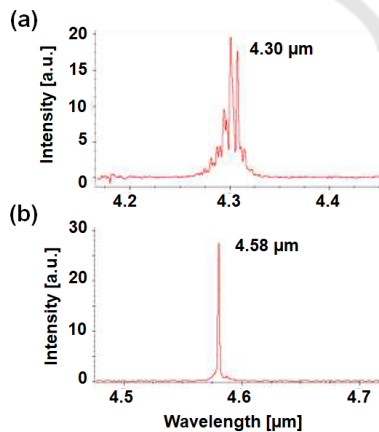


Figure 10: Measurement results of output wavelength. (a) baseline structure and (b) AlAs/InAs structure.

The lasing wavelength of baseline structure (A) was 4.52 μm, and that of improved structure (B) was 4.30 μm. In the simulation described in Chapter 3, the lasing wavelength of baseline structure (A) was 4.96 μm, and that of improved structure (B) was 4.77 μm.

The measurement results of baseline structure (A) and improved structure (B) were both 0.4 μm shorter than those in the simulation results. However, the improvement from baseline structure (A) to improved structure (B) enables us to reproduce the tendency for the lasing wavelength to become shorter.

5 CONCLUSIONS

We introduced a QCL laser simulator nextnano.QCL, which incorporates a nonequilibrium Green's function for calculating quantum effects. Assuming that the wavelength at which the gain is maximized is the laser oscillation wavelength, we compared the experimental oscillation wavelength in the reference with that in the simulation to confirm the validity of the simulator.

Furthermore, bandgap engineering was applied to the band structure of the QCL, and the following methods of increasing the power output of this structure were considered. Three types of structure were considered: (B) the AlAs/InAs structure that promotes the formation of a population inversion by promoting electron transport leakage, (C) the structure with a thin barrier layer that enhances electron transport, and (D) the structure with an active region with reduced Al composition that assists in the formation of population inversion. Using nextnano.QCL, the gains and wavelengths of these structures were calculated, and it was shown that the improved structure (B) had the highest gain. On the basis of simulation results, two types of QCL, baseline structure (A) and improved structure (B), were prototyped. The peak output of the laser with improved structure (B) was 1.73 times that with baseline structure (A). The validities of the method of pursuing high power output through bandgap engineering and simulation were demonstrated.

ACKNOWLEDGEMENTS

This work was supported by Innovative Science and Technology Initiative for Security (Grant Number JPJ004596), ATLA, Japan.

REFERENCES

Capasso F., 1987, "Band-Gap Engineering: From Physics and Materials to New Semiconductor Device, Science, 235, 172–176.

- Chaves A., Azadani J. G., Als Salman H., da Costa D. R., Frisenda R., Chaves A. J., Song S. H., Kim Y. D., He D., Zhou J., Castellanos-Gomez A., Peeters F. M., Liu Z., Hinkle C. L., Oh S.-H., Ye P. D., Koester S. J., Lee Y. H., Avouris P., Wang X., Low T., 2020, "Bandgap engineering of two-dimensional semiconductor materials", *npj 2D Materials and Applications*, 29, 1–21.
- Evans, A., Darvish, S. R., Slivken, S., Nguyen, J., Bai, Y., Razeghi, M., 2007. "Buried heterostructure quantum cascade lasers with high continuous-wave wall plug efficiency", *Appl. Phys. Lett.* 91, 071101.
- Faist J., Capasso F., Sivco D. L., Sirtori C., Hutchinson A. L., Cho A. Y., 1994. "Quantum cascade laser", *Science*, 264, 553–556.
- Faist J., Villares G., Scalari G., Rösch M., Bonzon C., Hugli A., Beck M., 2016. "Quantum Cascade Laser Frequency Combs", *Nanophotonics*, 5, 272–291.
- Grange, T., 2015. "Contrasting influence of charged impurities on transport and gain in terahertz quantum cascade lasers", *Phys. Rev. B*, 92, 241306-1–5.
- Hybertsen M. K., 1991, "Band offset transitivity at the INGAAS/InAlAs/InP(001) heterointerfaces", *Appl. Phys. Lett.* 58, 1759–1761.
- Lu S. L., Schrottke L., Teitsworth S. W., Hey R., Grahn H. T., 2006. "Formation of electric-field domains in GaAs/Al_xGa_{1-x}As quantum cascade laser structures", *Phys. Rev. B*, 73, 033311.
- Tanimura H., Takagi S., Kakuno T., Hashimoto R., Kaneko K., Saito S., 2022. "Analyses of Optical Gains and Oscillation Wavelengths for Quantum Cascade Lasers Using the Nonequilibrium Green's Function Method", *Journal of Computer Chemistry, Japan-International Edition*, 8, 0021–0024.